Supplemental information to ‘Quantifying the effect of salinity stratification on phytoplankton density patterns in estuaries’

Bo Liu, Huib E. de Swart

This document contains additional results of phytoplankton density (P) patterns for different boundary conditions and model parameters. In each experiment, one boundary condition or the value of one parameter is changed based on the setting of DF-W/DF-S (the default case for weakly/strongly stratified conditions). In all these experiments, P reaches equilibrium states within one week. Results are mainly presented by the values of ϕ_z and ϕ_x (defined in Eq. (20) and (21) of the main text), which quantify the overall vertical and along-estuary gradient of P at equilibrium, respectively.

S1 Setup of experiments

S1.1 Along-estuary turbulent diffusivity

A spatially constant longitudinal turbulent diffusivity κ_h was used in DF-W and DF-S. To examine the influence of the magnitude of κ_h on the values of ϕ_z and ϕ_x, experiments were conducted with the value of κ_h being halved and doubled, respectively, with respect to that of default cases. Moreover, experiments were further carried out with along-estuary varying κ_h, as shown in Fig. S1, to investigate the influence of the shape of κ_h on P pattern. Here, the values of κ_h were derived from the data of MacCready and Banas (2011), in which κ_h was treated as a fitting parameter to obtain the best representation of the measured tidal salt transport. Note that the data in MacCready and Banas (2011) are only available in the area $0 \leq x \leq 30$ km. In this area, the profiles were obtained by interpolating the data (open circles) of MacCready and Banas (2011). In the area $30 < x \leq 45$ km, the values of κ_h were obtained by extrapolating the data of MacCready and Banas (2011) with the constraint that $\kappa_h|_{x=45\ \mathrm{km}} = 2600\ \mathrm{m}^2\ \mathrm{s}^{-1}$. Here, the value $\kappa_h|_{x=45\ \mathrm{km}} = 2600\ \mathrm{m}^2\ \mathrm{s}^{-1}$ is chosen such that the along-estuary diffusive length scale $\sqrt{\kappa_h/\mu_{max}}$ is shorter than 15 km. This choice guarantees that the spatial distribution of P in $0 \leq x \leq 30$ km (within which area P patterns are presented and field data are available) is determined by internal dynamics rather than riverine boundary conditions.

S1.2 Tidally-averaged friction velocity and parameter A_S

In both DF-W and DF-S, the same value of the tidally-averaged friction velocity u_* was used as input in Eq. (8) for vertical eddy viscosity A_v. To investigate the sensitivity of the values of ϕ_z and ϕ_x to the value of this parameter, experiments were conducted with u_* reduced by a factor of 0.8 and increased by a factor of 1.2, respectively, with respect to its default value. The reason that u_* was not halved or doubled, as was done to other parameters, is because the amplitude of the density-driven flow u_d is inversely proportional to the overall intensity of A_v (see Eq. (3) and (4)). Halving u_* results in the magnitude of the subtidal current to be above 1 m s^{-1} under both weakly and strongly stratified conditions, which is unrealistic.

In the default cases DF-W and DF-S, the values of parameter A_S, which is proportional to the values of A_v and vertical eddy diffusivity κ_v at the water surface, has been tuned such that the amplitude and vertical structure of subtidal current are comparable to the field data of Chawla et al. (2008). Experiments were carried out with the value of A_S halved and doubled, respectively, with respect to those in the default cases.

S1.3 Bottom roughness length and river flow

The amplitude of the subtidal current decreases with increasing bottom roughness length z_0. The depth-averaged river flow U_r represents the river discharge, whose time series exhibit fluctuations as shown in Roegner et al. (2011). Here, experiments were conducted with the value of these two parameters halved and doubled, respectively, with respect to those in the default cases.

S1.4 Boundary conditions at the estuary mouth, phytoplankton and nutrient availability at the riverine boundary

In the default cases DF-W and DF-S, zero diffusive flux conditions have been imposed for P and N at the estuary mouth $x = 0$ (see Eq. (19)). A zero diffusive flux condition forces the along-estuary advection term to become zero at $x = 0$, as is shown in Fig. 8(g) and 8(h). To investigate the impact of this boundary condition on the values of ϕ_z and ϕ_x, experiments were conducted with the second derivatives of P and N with respect to x being zero at $x = 0$:

$$\left.\frac{\partial^2 P}{\partial x^2}\right|_{x=0} = 0, \quad \left.\frac{\partial^2 N}{\partial x^2}\right|_{x=0} = 0. \tag{S1}$$

To examine the influence of riverine phytoplankton and nutrient availability on the values of ϕ_z and ϕ_x, the density $P|_{x=L}$ and the nutrient concentration $N|_{x=L}$ at the riverine boundary $x = L$ were halved and doubled, respectively, with respect to their values in default cases.

S1.5 Parameters related to the loss rate, other than m_0

In the main text, the sensitivity of the values of ϕ_z and ϕ_x to the value of loss rate m_0 of phytoplankton in salt water, which parameterises the osmotic stress, has been presented and discussed. Here, sensitivity experiments concerning the other parameters in the parameterisation of the specific loss rate m (see Eq. (17)) are carried out. Specifically, The values of m_L (the value of loss rate of phytoplankton in fresh water), s_c (the salinity where $m = (m_0 + m_L)/2$) and s_δ (the salinity scale over which m varies) are halved and doubled, respectively, with respect to their values in default cases.

S1.6 Parameters that are not related to the loss rate in the biological module

The sensitivity of the values of ϕ_z and ϕ_x pattern to other biological parameters was investigated. To be specific, values of the following parameters were both halved and doubled with respect to those of default cases: the sinking velocity v of phytoplankton, the maximum specific growth rate μ_{max} of phytoplankton, the half-saturation constant of nutrient-limited growth H_N, the half-saturation constant of light-limited growth H_I, the light extinction coefficient k_{bg} due to background turbidity, the incident light intensity I_{in}, the light absorption coefficient k of phytoplankton, the nutrient amount α in each phytoplankton cell and the proportion ϵ of respired/grazed phytoplankton that is subsequently recycled.

S1.7 Effect of net growth of phytoplankton on P patterns

Finally, experiments were carried out in which the net growth of phytoplankton is completely switched off, that is, $(\mu - m) = 0$. These experiments were designed to test whether it is appropriate to treat phytoplankton as a tracer.

S2 Results and discussion

S2.1 Along-estuary turbulent diffusivity

Figure S2 shows the values of ϕ_z and ϕ_x for different values of spatially constant along-estuary turbulent diffusivity κ_h and for the along-estuary varying $\kappa_h = \kappa(x)$ (whose profiles are plotted in Fig. S1). Under weakly stratified conditions, ϕ_z hardly changes and ϕ_x slightly decreases with the magnitude of κ_h. This is because the along-estuary turbulent diffusion positively contributes to the accumulation rate of P in the lower reach ($0 < x < 10$ km), as is shown in Fig. 9(a). Thus, P in the lower reach increases with κ_h, and ϕ_x decreases accordingly.

Similarly, under strongly stratified conditions, ϕ_x slightly decreases with the magnitude of κ_h. However, the range over which ϕ_x varies is smaller compared to that during strong stratification because the along-estuary turbulent diffusion term is small, as is shown in Fig. 9(b).

When the along-estuary varying κ_h, which exhibits substantial fluctuations along the estuary (Fig. S1), is employed, ϕ_x slightly increases under both weakly and strongly stratified conditions. This is because the along-estuary diffusive transport is much weaker than the longitudinal advective transport induced by subtidal current, as is discussed in Section 4.1.

S2.2 Tidally-averaged friction velocity and parameter A_S

The values of ϕ_z and ϕ_x for different values of tidally-averaged friction velocity u_* and for different values of parameter A_S are shown in Fig. S3(a) and S3(b), respectively. If u_* is increased, the intensity of turbulence is increased. When the value of parameter A_S is increased, the values of vertical eddy viscosity and eddy diffusivity in the upper layer increases. Both the above changes amplify the negative contribution of the vertical turbulent diffusion to the accumulation rate of P in the upper layer, as is discussed in

Section 4.2.2. Thus, the values of ϕ_z decrease and those of ϕ_x increase.

S2.3 Bottom roughness length and river flow

Figure S4(a) shows values of ϕ_z and ϕ_x for different values of the bottom roughness length z_0. Under both weakly and strongly stratified conditions, the values of ϕ_z and ϕ_x hardly change with z_0 because halving or doubling the value of z_0 with respect to its default value causes only small changes in the amplitude of the subtidal current. Figure S4(b) shows values of ϕ_z and ϕ_x for different depth-averaged velocities U_r of river flow. During both weak and strong stratification, the value of ϕ_x decreases with increasing U_r because elevated U_r results in shorter time for phytoplankton being advected to the estuary mouth. Under strongly stratified conditions, the value of ϕ_z increases with increasing U_r because phytoplankton in the upper layer is subject to shorter period of sinking processes, as is discussed in Section 4.2.1.

S2.4 Boundary conditions at the estuary mouth, phytoplankton and nutrient availability at the riverine boundary

Figure S5(a) contains values of ϕ_z and ϕ_x for the experiments in which the second derivatives of P and N with respect to x vanish at the estuary mouth (see Eq. (S1)) and for those where zero along-estuary diffusive fluxes of P and N are imposed at the seaward boundary (see Eq. (19) for the default cases DF-W and DF-S). Under weakly stratified conditions, when Eq. (S1) is used, the value of ϕ_x slightly decreases compared to that for DF-W. This is because in the former case, the positive contribution of the along-estuary advection of P by subtidal current extends to the seaward boundary. As a result, P in the vicinity of the estuary mouth increases and the value of ϕ_x therefore decreases. During strong stratification, when Eq. (S1) is used, the value of ϕ_z slightly increases. This is because the positive contribution of the along-estuary advection term leads to the increase of P at the vicinity of the seaward boundary. However, the increase of P in the upper layer is much larger than that in the lower layer due to loss and sinking processes in the aphotic zone. Hence, the difference of P between the upper and the lower layer, as is measured by ϕ_z, is larger than that for DF-S.

Figure S5(b) shows values of ϕ_z and ϕ_x for different imposed values of phytoplankton density $P|_{x=L}$ at the riverine boundary. Under strongly stratified conditions, the value of ϕ_z decreases and that of ϕ_x increases with $P|_{x=L}$. As $P|_{x=L}$ increases, P in the interior of the estuary increases. Since high values of P occur in the upper layer during strong stratification, light is more limited for phytoplankton growth for larger $P|_{x=L}$. Hence, the specific net growth rate $(\mu - m)$ of phytoplankton in the upper layer generally decreases with increasing $P|_{x=L}$. As a result, P in the upper layer decreases, and accordingly the value of ϕ_z decreases with $P|_{x=L}$. Moreover, a decrease of $(\mu - m)$ further results in a faster decrease of P towards the estuary mouth, which leads to an increase of ϕ_x. Under weakly stratified conditions, the values of ϕ_z and ϕ_x hardly vary with $P|_{x=L}$. This is because P is vertically almost uniformly distributed rather than concentrated in the upper layer. Consequently, $(\mu - m)$ in the upper layer is hardly affected by the changes of light intensity due to varied $P|_{x=L}$ compared to that for strongly stratified conditions.

Figure S5(c) shows the values of ϕ_z and ϕ_x for different imposed nutrient concentrations $N|_{x=L}$ at the riverine boundary. Under strongly stratified conditions, the value of ϕ_z increases and that of ϕ_x decreases with $N|_{x=L}$. Similar to the spatial distribution of P at equilibrium, that of N (Fig. S6(b)) also shows a two-layer structure. In the upper layer, N is lower than $N|_{x=L}$ and generally decreases towards the estuary mouth due to consumption by phytoplankton. In the lower layer, N is much larger than $N|_{x=L}$ due to recycling of nutrient in dead phytoplankton cells. The N pattern indicates that nutrients are not efficiently exchanged between the upper and the lower layer. Hence, if the riverine nutrient availability is elevated, N in the upper layer in the interior of the estuary increases. As a result, $(\mu - m)$ in the upper layer becomes larger, which leads to an increase of ϕ_z and decrease of ϕ_x, as is discussed in the previous paragraph. Under weakly stratified conditions, the values of ϕ_z and ϕ_x hardly vary with $N|_{x=L}$. This is because during weak stratification, N is vertically mixed and generally increases towards the estuary mouth (see Fig. S6(a)), which indicates that N is sufficient for phytoplankton growth. Thus, increasing $N|_{x=L}$ results in little changes in $(\mu - m)$ and therefore negligible changes in the values of ϕ_z and ϕ_x.

S2.5 Parameters related to the loss rate, other than m_0

Figure S7(a) shows the values of ϕ_z and ϕ_x for different values of the loss rate m_L of phytoplankton in fresh water. Under strongly stratified conditions, the value of ϕ_z decreases and that of ϕ_x increases with increasing m_L. Values of P in the upper layer decrease with increasing m_L because an increase of the latter parameter results in a decrease of the net specific growth rate $(\mu - m)$ in the surface fresh water. As a consequence, ϕ_z decreases. The decreased $(\mu - m)$ in the surface fresh water further causes an increase of ϕ_x, as is discussed in Section S2.4. Under weakly stratified conditions, ϕ_z and ϕ_x hardly change with m_L. This is because m_L affect the loss rate in the fresh water area is $27 \leq x \leq 45$ km, whereas ϕ_z and ϕ_x quantify the characteristics of P pattern in the area $0 \leq x \leq 30$ km.

Figure S7(b) and S7(c) show the values of ϕ_z and ϕ_x for different values of s_c and s_δ, respectively. As s_c increases, for both weak and strong stratification, the value of ϕ_z hardly changes and that of ϕ_x slightly decreases. The changes in ϕ_x are because higher s_c values lead to smaller areas of high loss rates (see Eq. (17)), which results in less loss of P as phytoplankton are transported through the domain. The values of ϕ_z and ϕ_x hardly change for different values of s_δ within the range explored in this study.

S2.6 Biological parameters that are not related to the loss rate

Figure S8 shows the values of ϕ_z and ϕ_x for different sinking velocity v of phytoplankton. Under strongly stratified conditions, the value of ϕ_z decreases and that of ϕ_x increases with increasing v. An increased v leads to the decrease of P in the upper layer, as is illustrated by Fig. 8(h) and discussed in Section 4.1, and ϕ_z therefore decreases. Furthermore, along the estuary, P decreases faster towards the estuary mouth due to sinking processes, which results in the increase of ϕ_x. In the case of weakly stratified conditions, the ranges over which ϕ_z and ϕ_x vary are much smaller. This is because the sinking of phytoplankton has little impact if the vertical turbulent mixing is strong, as illustrated by Fig. 8(g). Note that ϕ_z falls below zero for $v = 2$ m day^{-1}, that is P at the estuary mouth attains higher values in the lower layer than in the upper layer.

Figure S9(a) shows the values of ϕ_z and ϕ_x for different values of maximum specific growth rate μ_{max}. As defined in Eq. (15), the specific growth rate μ of phytoplankton increases with μ_{max}. Thus, according to the discussion in Section S2.4, ϕ_z increases and ϕ_x decreases with μ_{max} under both weakly and strongly stratified conditions.

Figures S9(b) and S9(c) show the values of ϕ_z and ϕ_x for different values of half-saturation constant of nutrient-limited growth H_N and half-saturation constant of light-limited growth H_I, respectively. By increasing H_N (H_I), the specific growth rate μ of phytoplankton decreases. As a result, when increasing H_N (H_I), P patterns behave similar as those for decreasing μ.

The light extinction coefficient k_{bg} due to background turbidity and incident light intensity I_{in} are two parameters that influence light intensity in the water column. Fig. S10(a) shows the values of ϕ_z and ϕ_x for different values of k_{bg}. As k_{bg} increases, underwater light intensity decreases, which results in a decrease of the net specific growth rate $(\mu - m)$. Accordingly, under both weakly and strongly stratified conditions, ϕ_z decreases and ϕ_x increases with k_{bg}, as discussed in Section S2.4. Similar to a increase in k_{bg}, a decrease in incident light intensity I_{in} also cause stronger limitation on the growth of phytoplankton. Accordingly, ϕ_z decreases and ϕ_x increases with I_{in}, as is shown in Fig. S10(b).

Figure S10(c) contains the values of ϕ_z and ϕ_x for different light absorption coefficient

k of phytoplankton. Similar to increasing background turbidity k_{bg}, increasing k also leads to decrease of light intensity in the water column. Thus, ϕ_z decreases and ϕ_x increases with k.

Figure S11(a) and S11(b) show the values of ϕ_z and ϕ_x for different nutrient amount α in each phytoplankton cell and nutrient recycling coefficient ϵ, respectively. Clearly, both ϕ_z and ϕ_x hardly change with either α or ϵ. This is because during weak stratification, the values of ϕ_z and ϕ_x are not sensitive to the changes of nutrient concentration N, as is illustrated by Fig. S5(c) and discussed in Section S2.4. Under strongly stratified conditions, for different values of α or ϵ used in this study, the values of N in the upper layer changes in a small range such that the net specific growth rate $(\mu - m)$ is hardly affected.

S2.7 Effect of net growth of phytoplankton on P patterns

Figure S12 shows the spatial distribution of P at equilibrium for the experiment in which the net growth of phytoplankton is switched off, i.e., $(\mu - m) = 0$. Clearly, under both weakly and strongly stratified conditions, P values are high in the domain and they increases towards the bottom. These patterns are markedly different from those of the default cases DF-W and DF-S, as well as from the observed P patterns shown by Roegner et al. (2011).

References

Chawla, A., Jay, D. A., Baptista, A. M., Wilkin, M., Seaton, C., 2008. Seasonal variability and estuary-shelf interactions in circulation dynamics of a river-dominated estuary. Estuaries and Coasts 31, 269–288.

MacCready, P., Banas, N. S., 2011. Residual circulation, mixing, and dispersion. In:

Wolanski, E., McLusky, D. S. (Eds.), Treatise on Estuarine and Coastal Science. Vol. 2. Elsevier, Waltham, pp. 75–89.

Roegner, G. C., Seaton, C., Baptista, A. M., 2011. Climatic and tidal forcing of hydrography and chlorophyll concentrations in the Columbia River estuary. Estuaries and Coasts 34, 281–296.

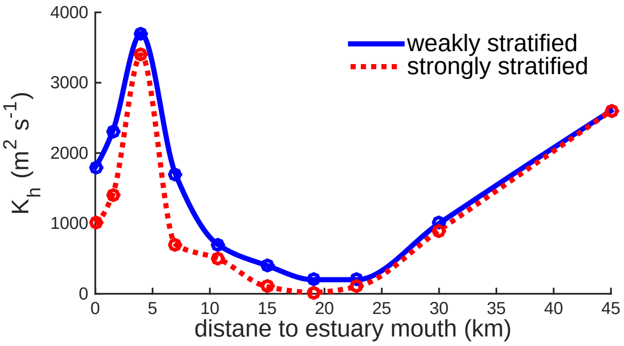

Figure S1: The along-estuary profiles of along-estuary turbulent diffusivity κ_h for weakly stratified conditions (solid line) and strongly stratified conditions (dotted line). In the area $0 \leq x \leq 30$ km, the profiles were obtained by interpolating the data (open circles) of MacCready and Banas (2011). In the area $30 < x \leq 45$ km, the profiles were obtained by exterpolating the data of MacCready and Banas (2011) with the constraint that $\kappa_h|_{x=45 \text{ km}} = 2600 \text{ m}^2 \text{ s}^{-1}$

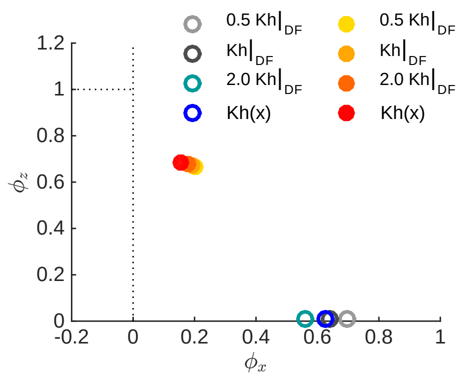

Figure S2: Scatter plot of ϕ_z and ϕ_x for different values of spatially constant along-estuary turbulent diffusivity κ_h, and also for along-estuary varying κ_h as shown in Fig. S1. Here, open circles indicate results for weakly stratified conditions, whereas full circles represent results for strongly stratified conditions.

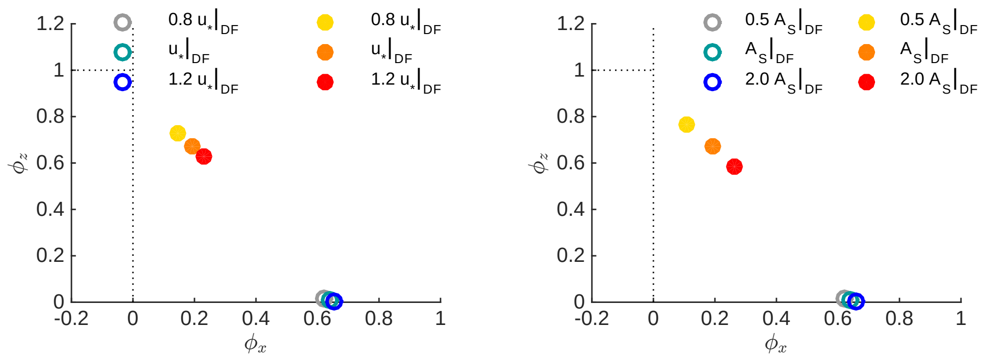

(a) (b)

Figure S3: As Fig. S2, but (a) for different values of the tidally averaged friction velocity u_* and (b) for different values of parameter A_S (that is proportional to the values of vertical eddy viscosity and eddy diffusivity at the water surface)

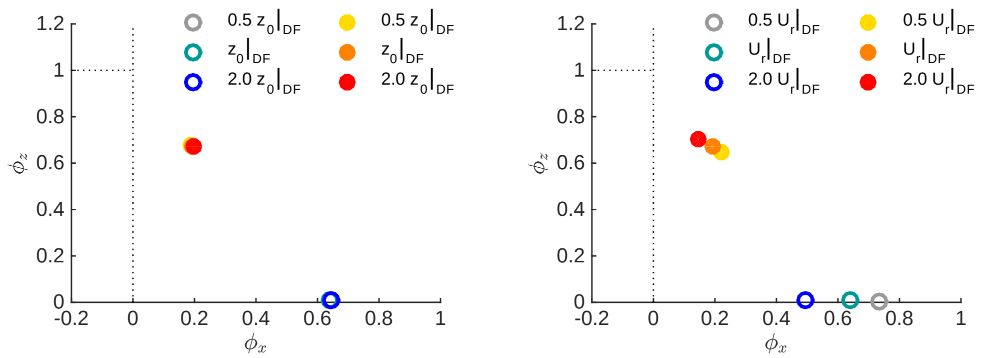

(a) (b)

Figure S4: As Fig. S2, but (a) for different values of the bottom roughness length z_0 and (b) for different values of depth-averaged velocity U_r of river flow

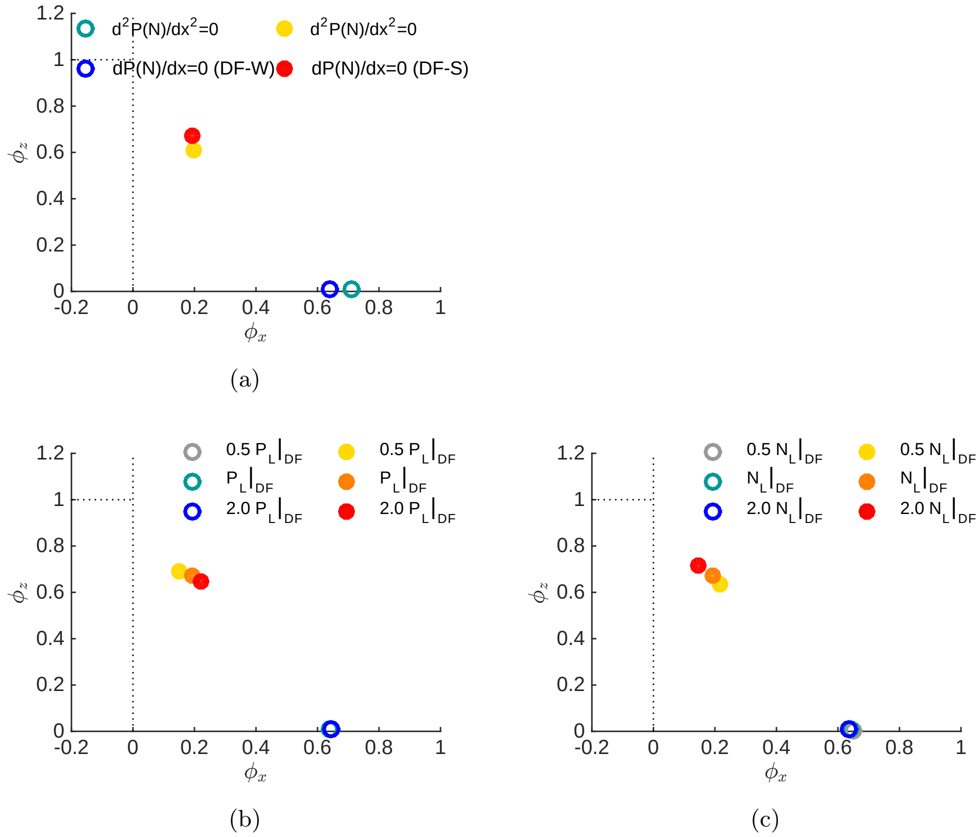

Figure S5: As Fig. S2, but (a) for different boundary conditions of P and N at the estuary mouth $x = 0$, (b) for different values of phytoplankton density $P|_{x=L}$ at the riverine boundary $x = L$ and (c) for different values of nutrient concentration $N|_{x=L}$ at $x = L$

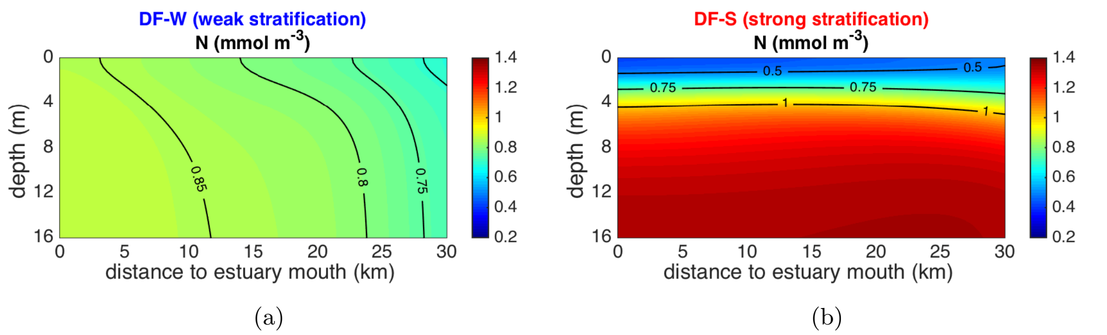

Figure S6: (a), (b): Spatial distribution of nutrient concentration N at equilibrium for DF-W and DF-S, respectively

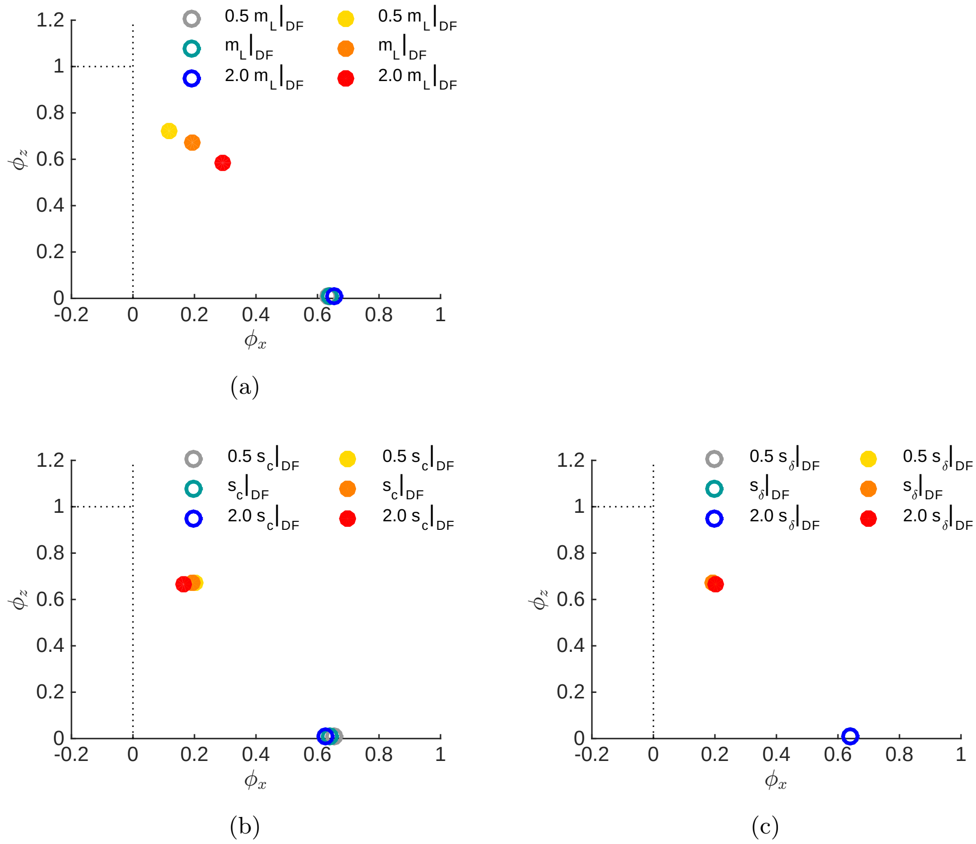

Figure S7: As Fig. S2, but (a) for different values of the loss rate m_L of phytoplankton in fresh water, (b) for different values of s_c (the salinity at which $m = (m_0 + m_L)/2$) and (c) for different values of s_δ (the salinity scale over which m varies)

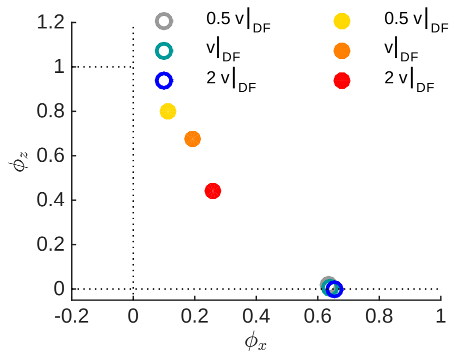

Figure S8: As Fig. S2, but for different values of the sinking velocity v of phytoplankton

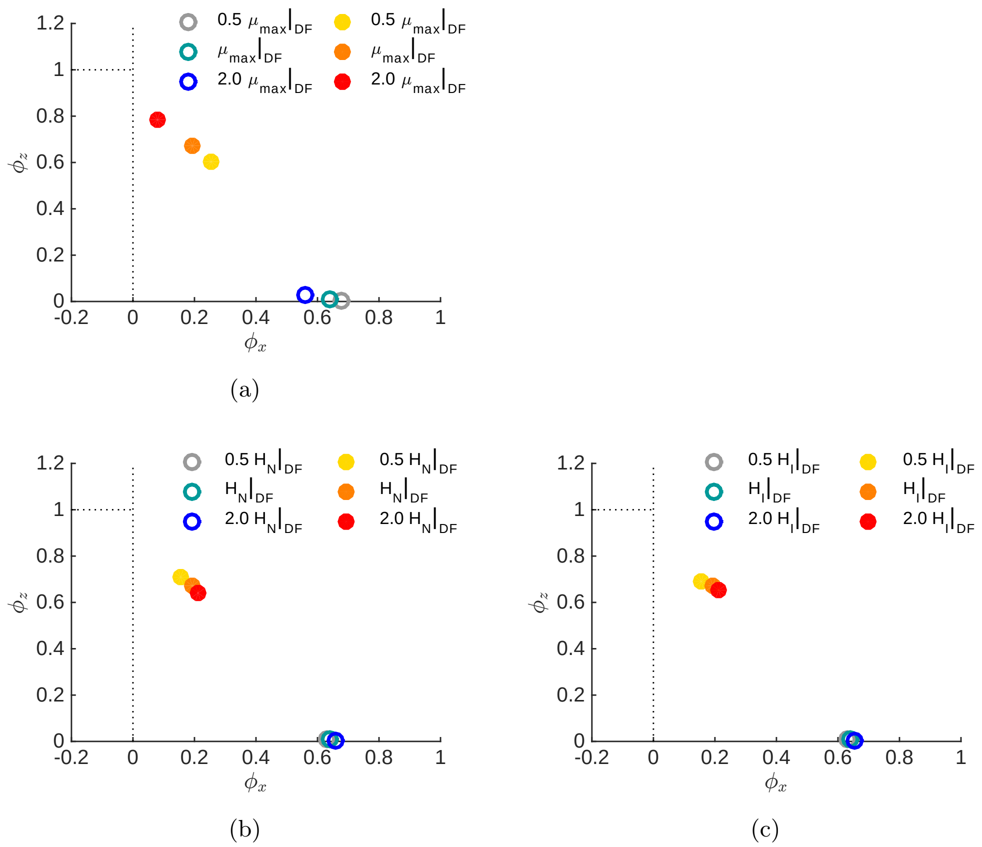

Figure S9: As Fig. S2, but (a) for different values of the maximum specific growth rate μ_{max} of phytoplankton, (b) for different values of the half-saturation constant H_N of nutrient-limited growth and (c) for different values of the half-saturation constant H_I of nutrient-limited growth

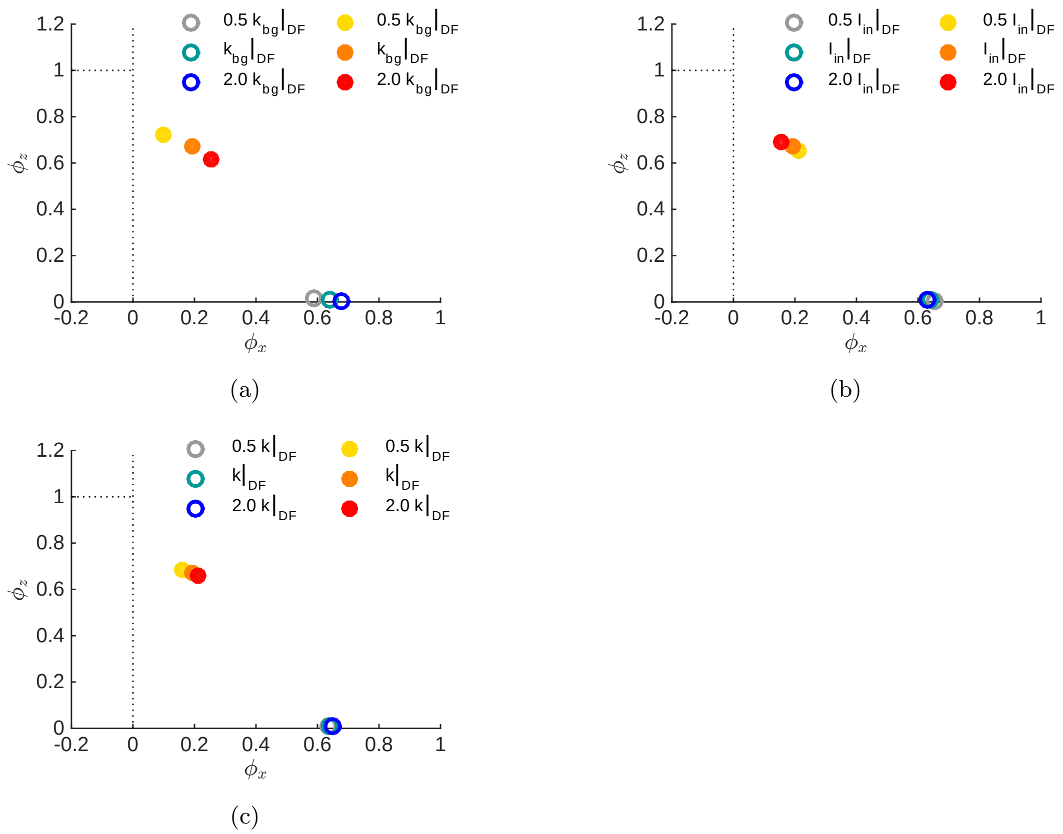

Figure S10: As Fig. S2, but (a) for different values of the light extinction coefficient k_{bg} due to background turbidity, (b) for different values of the incident light intensity I_{in} and (c) for different values of the light absorption coefficient k of phytoplankton

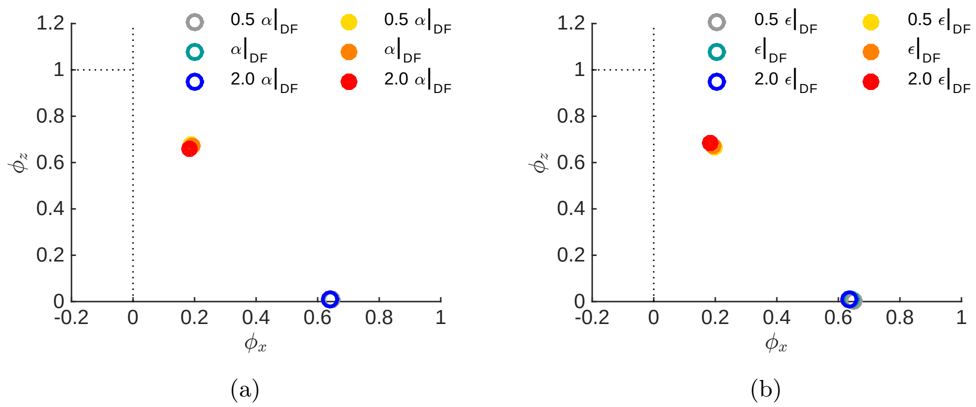

Figure S11: As Fig. S2, but (a) for different values of the nutrient amount α in each phytoplankton cell and (b) for different values of the nutrient recycling coefficient ϵ

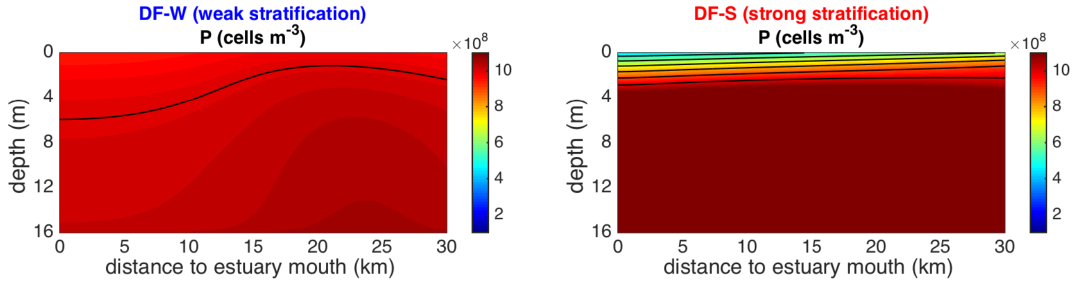

(a) (b)

Figure S12: Spatial distributions of phytoplankton density P at equilibrium for the experiments, in which the net growth of phytoplankton is switched off, that is $(\mu - m) = 0$, under (a) weakly stratified conditions and (b) strongly stratified conditions